Electronic Supplementary Material (ESI) for Analyst.
This journal is © The Royal Society of Chemistry 2023
Electronic Supplementary Material (ESI) for Analyst. This journal is © The Royal Society of Chemistry 2023

# Electronic Supplementary Material

# Electrodeposition of paracetamol oxide for intelligent portable ratiometric detection of nicotine and ethyl vanillin β-D-glucoside

Zhaohong Su,[ab] Shiyu Hu,[b] Yuhang Zhang,[b] Zhanning Liang,[b] Yi Peng,[b] Qinyi Cao,[b] Xia Yu,[b] Zhiyang Zhu,*[a] Pei He*[a] and Zhenjie Li*[a]

[a] Yunnan Key Laboratory of Tobacco Chemistry R&D Center of China Tobacco Yunnan Industry Co., Ltd. 650231 Kunming, PR China.

[b] College of Chemistry and Materials Science, College of Agronomy, Hunan Agricultural University, Changsha 410128, PR China.

*Corresponding author. Tel.: +86 871 65869792; Fax: +86 871 65869792.

E–mail address: fly10080704@163.com (Zhiyang Zhu); hepeisuccess@163.com (Pei He); kmlizhenjie@163.com (Zhenjie Li)

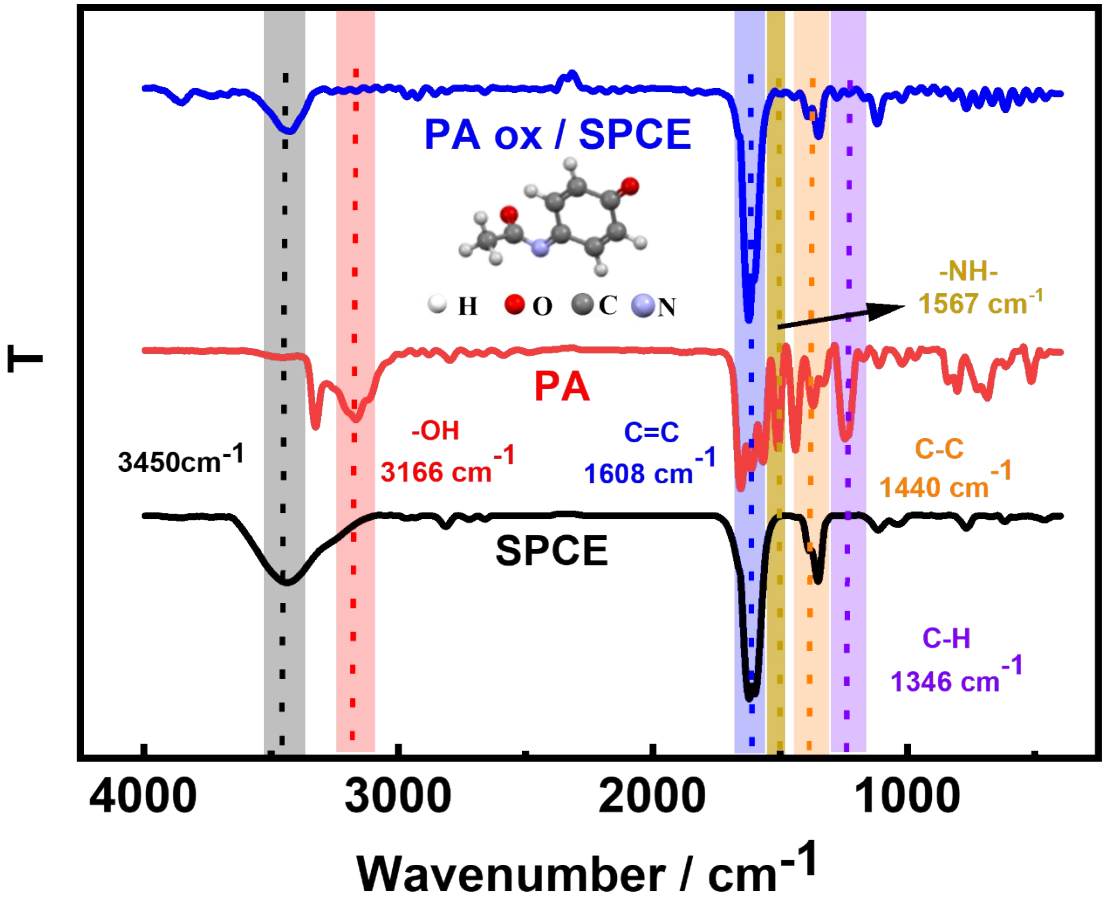


**Fig. S1.** FT-IR spectra of PA ox / SPCE, PA and SPCE.

Fig. S1 shows FT-IR spectra of PA at 3325 $cm^{-1}$ (N-H amide stretching), 3166 $cm^{-1}$ (free-OH stretching), 1654 $cm^{-1}$ (C=O stretching), 1608 $cm^{-1}$ (C=C stretching), 1567 $cm^{-1}$ (N-H amide II bending), 1509 $cm^{-1}$ (asymmetric C-H bending), 1440 $cm^{-1}$ (C-C stretching), 1368-1328 $cm^{-1}$ (C-H symmetric bending) and 1260-1227 $cm^{-1}$ (C-N stretching)[1]. The peak intensity at 3450 $cm^{-1}$ of PA ox / SPCE is lower than that of SPCE, and the characteristic peaks of PA appear in PA ox / SPCE at 3166 $cm^{-1}$, 1608 $cm^{-1}$, 1440 $cm^{-1}$, the characteristic peak of PA at 1567 $cm^{-1}$ was oxidized to =N- under electrodeposition, so the characteristic peak of N-H could not be observed on PA ox/SPCE. so it is speculated that PA has been electrodeposited successfully on SPCE. This result is consistent with EDS (Fig. 2c and Fig. 2d).

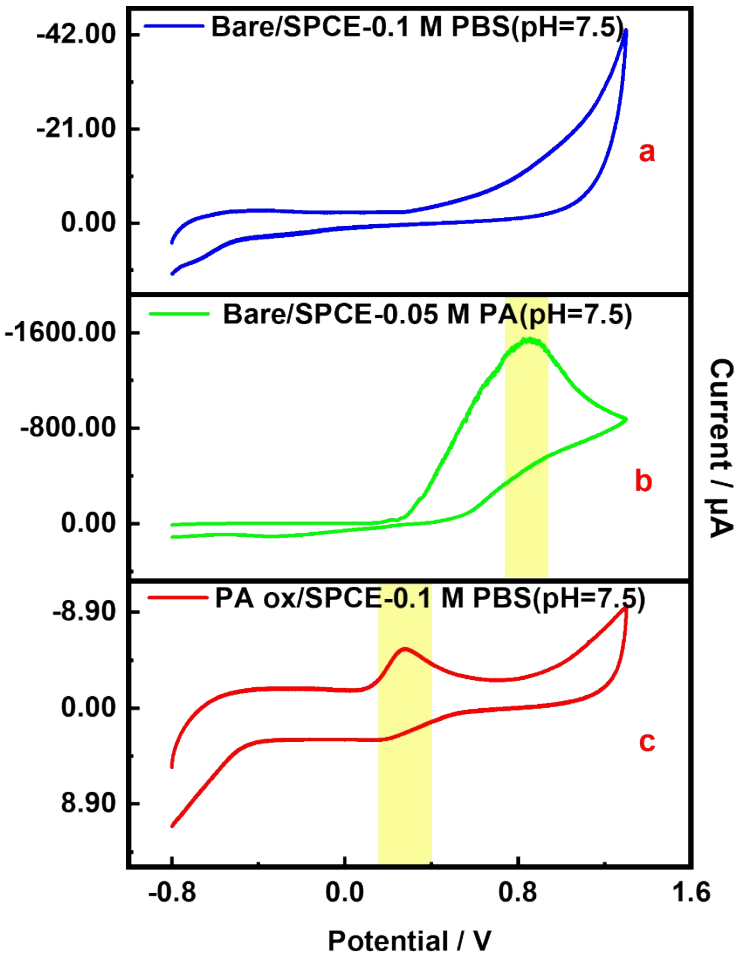


**Fig. S2.** (a) CV of SPCE in 0.1 M PBS (pH=7.5). (b) CV of SPCE in 0.1 M PBS (pH=7.5) containing 0.05 M PA. (c) CV of PA ox/SPCE in 0.1 M PBS (pH=7.5). Scan rate: 100 mV $s^{-1}$.

Compared with Fig. S2a, Fig. S2b shows that SPCE has a large oxidation peak and peak potential difference in 0.1 M PBS (pH=7.5) containing 0.05 M PA solution. It is worth noting that Fig. S2c was characterized by CV in phosphate buffer (pH=7.5) after electrodeposition of PA ox. It is found that both the peak potential difference and the oxidation peak current decrease, and it is further speculated that only a small amount of PA oxidation products are deposited on the electrode surface.

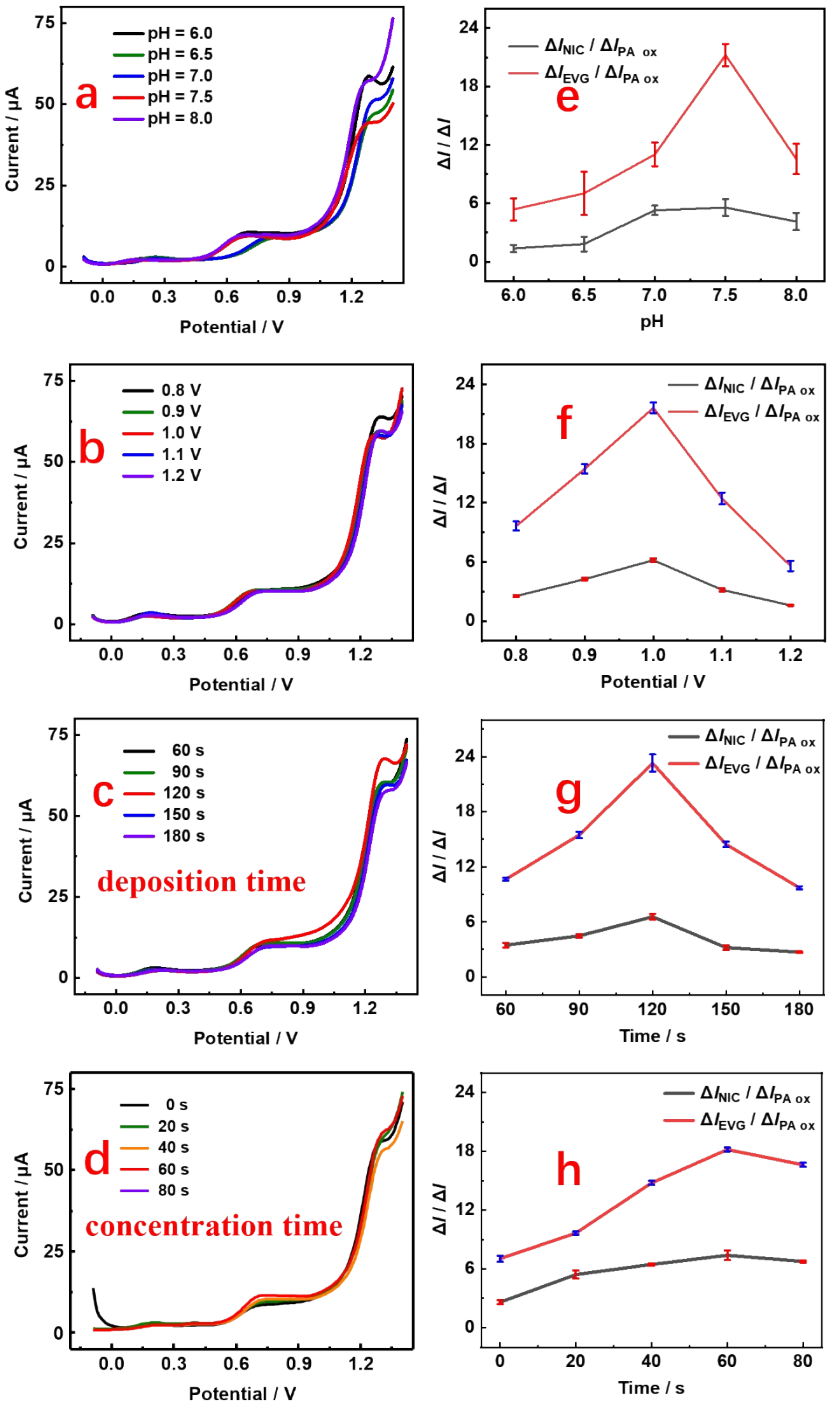


**Fig. S3.** SWV curves of PA ox/SPCE in 0.1 mol/L PBS containing 60 μmol/L NIC and 60 μmol/L EVG with different pH values (a), different PA deposition potentials (b), different PA deposition time (c) and different enrichment time (d). Effects of pH (e), PA deposition potential (f), PA deposition time (g) and enrichment time (h) on ratiometric current of sensor.

Optimization of determination conditions of PA ox / SPCE. According to the SWV peak current ratio of PA ox / SPCE in 0.1 mol/L PBS containing 60 μmol/L NIC and 60 μmol/L EVG, it can be obtained that when pH=7.5, PA ox / SPCE has the largest response to NIC and EVG. The deposition potential of PA was optimized by five potential values in Figs. S3(b, f). It can be seen from Figs. S3 (b, f) that when the deposition potential is 1 V, the SWV peak current ratio of PA ox / SPCE is the largest. Figs. S3 (c, g) shows the optimization of PA deposition time. When the deposition time is 120 s, the SWV peak current ratio of PA ox / SPCE is the largest. The optimization of the detection enrichment time is shown in Figs. S3 (d, h). From Fig. S3h, it can be seen that when the enrichment time is 60 s, PA ox / SPCE has the greatest influence on the SWV peak current ratio of NIC and EVG. The optimization of these detection conditions were carried out to obtain the best detection conditions, and the subsequent experiments were selected under the best conditions.

**Table S1** Comparison of simultaneous detection and ratiometric simultaneous detection mode

| Method | Detection substance | Linear functions | $R^2$ | LR(μM) | LOD(μM) |
|---|---|---|---|---|---|
| simultaneous detection | NIC | $y=0.09136C_{NIC}-2.87321$ | 0.9929 | 30-80 | 0.98 |
| | EVG | $y=0.20617C_{EVG}-6.4661$ | 0.9562 | 30-80 | 0.088 |
| ratiometric simultaneous detection | NIC | $y=0.11231C_{NIC}-1.00027$ | 0.9983 | 10-200 | 0.256 |
| | EVG | $y=0.38657C_{EVG}-3.42956$ | 0.9945 | 10-180 | 0.058 |

**Table S2*** Comparison of sensing properties of nicotine electrochemical detection.

| Electrodes | ratiometric sensor | Detection substance | Linear range/μmol/L | Detection Limit/μmol/L | Supporting electrolyte | Ref. |
|---|---|---|---|---|---|---|
| CS/MWCNT-COOH | No | NIC | 0.1-100 | 30 | 0.1 M PBS (pH 7.4) | [2] |
| BDDE | No | NIC | 0.03-0.40 | 0.01 | 0.1 M $NH_3$-$NH_4Cl$ (pH 7.5) | [3] |
| BN/graphene/GCE | No | NIC | 1 - 1000 | 0.42 | 0.1 M PBS (pH 7) | [4] |
| PEDOT/GR/GCE | No | NIC | 0.5-1000 | 0.047 | 0.1 M PBS (pH 7) | [5] |
| ERCG/GCE | No | NIC | 2-5, 2-60 | 0.1 | 0.1 M PBS (pH 7.0) | [6] |
| GO-4-ATP-Au-PT/Au GCE | No | NIC | 1-30 | 0.17 | 0.1 M PBS (pH 7.0) | [7] |
| GO/Nq/GCE | No | NIC | 6.5-245 | 12.7 | 0.1 M PBS (pH 7.0) | [8] |
| PDA-RGO/Au | No | NIC | 0.05-500 | 0.015 | 0.1 M BR (pH 7.5) | [9] |
| GC/NfMWCNTs/Fe$(bpy)_3^{2+}$ | No | NIC | 0.1-3000 | 0.1 | 0.1 M PBS (pH 4.5) | [10] |
| PA ox / SPCE | Yes | NIC<br>EVG | 10-200<br>10-180 | 0.256<br>0.058 | 0.1 M PBS (pH 7.5) | This work |

*CS/MWCNT-COOH: Carbon nanotube hybrid nanofibers, BDDE: boron-doped diamond electrode, BN/graphene/GCE: hexagonal boron nitride doped graphene, PEDOT/GR/GCE: graphene/poly(3,4-ethylenedioxythiophene) nanocomposite ERCG: electroreduced carboxylated graphene, GO-4-ATP-Au-PT/Au: graphene oxide-4-aminothiophene-Au nanoparticle-polythiophene/Au nanoparticle, GO/Nq/GCE: 1,2-naphthoquinone-4-sulfonic acid conjugated graphene oxide nanoparticles, PDA-RGO/Au: Polydopamine functionalized reduced graphene oxide-gold nanoparticle, GC/Nf-MWCNTs/Fe-$(bpy)_3^{2+}$: Nafion-multiwalled carbon nanotubes supported bipyridyl Iron (II).

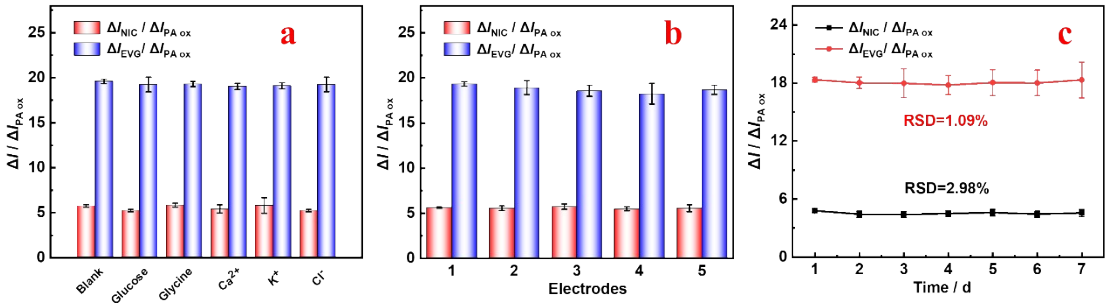


**Fig. S4.** (a) Ratiometric anode peak current of PA ox / SPCE in 0.1 mol/L PBS (pH=7.5) containing 60 μmol/L NIC, 60 μmol/L EVG and different interfering substances (5 mmol/L Glucose and Glycine; 1 mmol/L $Ca^{2+}$, $K^{+}$ and $Cl^{-}$). (b) Ratiometric anode peak current of five PA ox / SPCE electrodes in 0.1 mol/L PBS (pH=7.5) containing 60 μmol/L NIC and 60 μmol/L EVG. (c) Ratiometric anode peak current of PA ox / SPCE in 0.1 mol/L PBS (pH=7.5) containing 60 μmol/L NIC and 60 μmol/L EVG from 1 day to 7 days.

Anti-interference, repeatability and stability of PA ox/SPCE sensor. As shown in Fig. S4, in order to determine the applicability and stability of PA ox / SPCE in the real detection, the following three tests were performed. Fig. S4a performed anti-interference experiments on common components of cigarettes, and selected substances that may be contained as interferences. The effects of glucose, glycine, $Ca^{2+}$, $K^{+}$ and $Cl^{-}$ on PA ox/SPCE detection[11]. The experimental results show that $\Delta I_{NIC}/\Delta I_{PA}$ and $\Delta I_{EVG}/\Delta I_{PA}$ are similar to the blank test results, and the small changes can be ignored. In order to clarify the reproducibility of PA ox / SPCE, five PA ox / SPCE (Fig. S4b) were prepared, and the effects of different electrodes on $\Delta I_{NIC}/\Delta I_{PA}$ and $\Delta I_{EVG}/\Delta I_{PA}$ are not obvious. In order to clarify the stability of PA ox / SPCE, PA ox / SPCE was stored in a refrigerator for 7 days to study its long-term stability (Fig.

S4c). Similarly, $\Delta I_{NIC}/\Delta I_{PA}$ and $\Delta I_{EVG}/\Delta I_{PA}$ remain relatively stable, and the RSD for $\Delta I_{NIC}/\Delta I_{PA}$ and $\Delta I_{EVG}/\Delta I_{PA}$ is 2.89% and 1.09%, respectively, indicating that the proposed PA ox / SPCE has good stability.

**Table S3*** Comparison of simultaneous electrochemical detection characteristics of nicotine in different literatures.

| Materials/electrodes | Detection Method | Detection substance | Potential (V) | Linear range (μM) | Detection limit (μM) | Reference |
|---|---|---|---|---|---|---|
| ZnO/3,4'AAZCPE | SWV | Ne<br>NIC | 0.82 | 2500-5000 | - | [13] |
| PtBA/AuNPs/GC | DPV | Tyr<br>Tyr<br>NIC | 0.90 | 0.02-300 | 0.93 | [14] |
| HA-GH-MWCNT/GCE | SWV | Caffeine<br>NIC | 0.97 | 22.35-169.35 | 1.19 | [15] |
| $MgNi_{1.95}Fe_{0.05}O_3$/GCE | SWV | DA<br>UA<br>NIC | 0.86 | 50-4000 | 0.098 | [16] |
| CuNC@N-GQds | DPV | CA<br>DA<br>NIC | 0.10 | 0.00001-1 | 0.01 | [17] |
| PA ox / SPCE | SWV | SER<br>EVG<br>NIC | 0.72 | 10-200 | 0.256 | This work |

*ZnO/3,4'AAZCPE:ZnO nanorods and 3-(4'-amino-3'-hydroxy-biphenyl-4-yl)acrylic acid; PtBA/AuNPs/GC: a taurine (Tau) and reactive blue 4 (RB4) bonded-conducting polymer(poly (2,2′:5′,5″-Terthiophene-3′-p-benzoic acid)layer formed on AuNPs doped-glassy carbon; HA-GH-MWCNT/GCE: ternary hydroxyapatite-graphenemulti-walled carbon nanotube nanocomposite; $MgNi_{1.95}Fe_{0.05}O_3$/GCE: 2.5 wt% Fe doped $MgNi_2O_3$ nanoparticles modified glassy carbon electrode; CuNC@N-GQds: CuNC on nitrogen-doped graphene quantum dots.

**Reference** (only for Electronic Supplementary Material)


1. Z. I. Yildiz and T. Uyar, *Appl. Surf. Sci.*, 2019, **492**, 626-633.
2. A. Mirani, L. Maleknia and A. Amirabadi, *Nanotechnology*, 2020, **31**.
3. M. Kowalcze and M. Jakubowska, *Diamond Relat. Mater.*, 2020, **103**, 107710.
4. R. Jerome and A. K. Sundramoorthy, *Anal. Chim. Acta*, 2020, **1132**, 110-120.
5. J. Rajendran, A. N. Reshetilov and A. K. Sundramoorthy, *Materials Advances*, 2021, **2**, 3336-3345.
6. H. Xiao, L. Sun, H. Yan, W. Wang, J. Liu, Q. Yan, L. Chao, C. Chen, Q. Xie, J. Wen and D. Yin, *Anal. Methods*, 2015, **7**, 1147-1153.
7. A. Saljooqi, T. Shamspur and A. Mostafavi, *J. Mater. Sci.: Mater. Electron.*, 2020, **31**, 5471-5477.
8. M. Abd-Elsabour, H. M. Alsoghier, A. G. Alhamzani, M. M. Abou-Krisha, T. A. Yousef and H. F. Assaf, *Nanomaterials*, 2022, **12**.
9. Y. Jing, X. Yuan, Q. Yuan, K. He, Y. Liu, P. Lu, H. Li, B. Li, H. Zhan and G. Li, *Sci Rep*, 2016, **6**, 29230.
10. A. Tiwari, M. Yadav, D. Kumar Singh and V. Ganesan, *Electroanalysis*, 2022, **35**.
11. G. Sridharan, K. L. Babu, D. Ganapathy, R. Atchudan, S. Arya and A. K. Sundramoorthy, *Crystals*, 2023, **13**, 589.
12. Y. Lin, L. Liu, G. Ou, W. Huang and K. Wu, *Anal. Chim. Acta*, 2023, **1249**, 340907.
13. E. Molaakbari, A. Mostafavi and H. Beitollahi, *Electroanalysis*, 2014, **26**,

2252-2260.

14. W.-C. Lee, H.-B. Noh, K. K. Hussain, S.-J. Min and Y.-B. Shim, *Sensors and Actuators B: Chemical*, 2018, **275**, 284-291.

15. Sudhan, Lavanya, Leonardi, Neri and Sekar, *Sensors*, 2019, **19**.

16. S. L. Reddy, C. Arul, L. Zhaoqi, N. Lavanya and C. Sekar, *J. Electroanal. Chem.*, 2020, **878**.

17. S. S, A. N. J. S and S. K. Y, *Journal of Materials Chemistry B*, 2022, **10**, 3974-3988.